

Short-term dynamics of late-winter phytoplankton blooms in a temperate ecosystem (Central Cantabrian Sea, Southern Bay of Biscay)

EVA ÁLVAREZ^{1*}, ENRIQUE NOGUEIRA¹, JOSÉ LUIS ACUÑA², MARCOS LÓPEZ-ÁLVAREZ² AND JORGE A. SOSTRES²

¹INSTITUTO ESPAÑOL DE OCEANOGRAFÍA, CENTRO OCEANOGRÁFICO DE GIJÓN, 33212 GIJÓN, SPAIN AND ²ÁREA DE ECOLOGÍA, DEPARTAMENTO DE BIOLOGÍA DE ORGANISMOS Y SISTEMAS, FACULTAD DE BIOLOGÍA, UNIVERSIDAD DE OVIEDO, 33006 OVIEDO, SPAIN

*CORRESPONDING AUTHOR: eva.alvarez@gi.ieo.es

Received November 28, 2008; accepted in principle January 22, 2009; accepted for publication January 24, 2009

Corresponding editor: William Li

The Spring Phytoplankton Bloom takes place in the Central Cantabrian Sea (Southern Bay of Biscay) from late-winter to spring as a series of blooms with variable biomass accumulation. In late-winter of 2004 and 2005, phytoplankton blooms occurred in this area following a change in the weather. In order to describe the dynamics of these late-winter blooms, two oceanographic cruises which involved high-frequency sampling (every 2–3 days) were carried out. Meteorological conditions during the cruises showed similar changes in variables relevant to phytoplankton physiology and population dynamics. Before the bloom, phytoplankton started to grow actively when underwater photosynthetic active radiation (PAR) increased. However, biomass accumulation did not occur until wind, and hence turbulence levels in the water column, decreased. The observations presented here suggest that before the onset of a late-winter bloom a preliminary physiological activation phase is necessary driven by increased availability of underwater PAR. Afterwards, biomass accumulation can take place provided wind-derived water column turbulence decays. The development of the bloom is reinforced by the shoaling of the surface mixing layer depth. The timing of this sequence of events can be altered by meteorological disturbances, such as an increase of wind speed. The composition of the bloom differed across-shelf: phytoplankton larger than 5 μm in equivalent spherical diameter (ESD) dominated on the coast and inner shelf, whereas smaller phytoplankton (<5 μm ESD) were more important in the oceanic area, markedly when a frontal structure separating both domains developed at the mid-shelf.

INTRODUCTION

The study of the factors and mechanisms underlying the variability of phytoplankton populations is a pervading theme in marine ecology. It is widely recognized that bottom-up processes, driven ultimately by meteorological-hydrographic variability, play a major role in the control and modulation of phytoplankton populations (e.g. Smayda, 1998; Nogueira *et al.*, 2000). Consequently, the study of the environmental conditions favouring population increase, decrease or maintaining

a constant population is an important line of research in order to understand the large temporal and spatial variability that occurs in the distribution of phytoplankton.

The Cantabrian Sea (Southern Bay of Biscay) belongs to the Northeast Atlantic Shelves Province (Longhurst, 1998). Accordingly, its seasonality corresponds to a temperate sea, characterized by four main oceanographic seasons that define the main points in relation to the annual cycle of phytoplankton biomass

and seasonal succession: (i) a relatively intense mixing period in winter, when the replenishment of nutrients to the surface layers occurs but phytoplankton biomass is low due to light-limitation; (ii) the development of the seasonal thermocline at the beginning of spring, characterized by intense nutrient uptake associated with phytoplankton growth; (iii) the consolidation of thermal stratification during summer, when surface nutrient concentrations reach minimum annual values and thus limit phytoplankton production and (iv) a de-stratification phase in autumn (Varela, 1996), when another phytoplankton bloom may occur during the transitional stage between stratification and mixing (Fernández and Bode, 1991). However, as can be deduced from satellite images (Ueyama and Monger, 2005), phytoplankton blooms framed within this annual scenario usually take place as short-lived events that persist for only 1 to 2 weeks.

A bloom can be defined as a rapid increase of phytoplankton biomass caused by locally enhanced primary production (Legendre, 1990). This definition focuses on two necessary features of a bloom: the enhancement of primary production and the accumulation of phytoplankton biomass. Mechanisms underlying bloom initiation have been an important focus of interest since the 1930s (Gran and Braarud, 1935). Historically, the hypotheses about bloom development have tried to explain bloom dynamics invoking a unique mechanism and exploring which physical factors govern these dynamics at the community level. The best-studied example of such proliferations is the Spring Phytoplankton Bloom in temperate and sub-polar waters, whose occurrence is explained by models focusing on the need to keep cells in the illuminated zone of the water column (Riley, 1942; Sverdrup, 1953; Huisman *et al.*, 1999). The critical depth hypothesis (Sverdrup, 1953) focuses on the relationship between the compensation depth, where gross primary production and respiration are balanced, and the surface mixed layer depth (MLD), within which phytoplankton is mixed up and down. It predicts that when the MLD becomes shallower than a certain critical value (critical depth, z_{cr}), phytoplankton cells are retained in the upper illuminated part of the water column above the compensation depth, receiving enough photosynthetic active radiation (PAR) to make gross primary production during the day exceed losses due to respiration and hence allowing bloom development. Alternatively, as Sverdrup pointed out in his seminal paper (Sverdrup, 1953), a phytoplankton population can increase independently of the MLD provided turbulence is low enough to keep cells in the illuminated surface layer (i.e. critical turbulence hypothesis; Huisman *et al.*, 1999).

Thus, either turbulence is intense and a shallowing of the MLD is necessary to expose phytoplankton to favourable light conditions, or turbulence is weak, independently of the MLD, and phytoplankton net growth rate exceeds vertical mixing rate. This last situation has been observed in the North Atlantic (Townsend *et al.*, 1992; Eilertsen, 1993) and the North Sea (Backhaus *et al.*, 1999; Dale *et al.*, 1999), and it seems to have been observed in the North and Northwest shelf waters of the Iberian Peninsula (Fernández and Bode, 1991).

However, some authors maintain that these mechanisms of bloom initiation do not adequately explain the onset of the bloom (Smetacek and Passow, 1990) and have limited value as a diagnostic tool (Platt *et al.*, 1991). Diatoms, usually the dominant component of the Spring Phytoplankton Bloom (Varela, 1996), are present in the winter community, although their metabolic rates must be low due to light limitation. When conditions turn out to be favourable, i.e. light limitation relaxes, they are capable of fast growth. Given the different time scale between the whole winter and a bloom event, it seems that environmental conditions during late-winter/early-spring select those species which are capable of achieving high growth rates. So, it is necessary to introduce some physiological criteria at the individual level in bloom initiation to explain this change between maintenance and growth metabolism (Smetacek and Passow, 1990). The Sverdrup critical depth criterion and, consequently, the Huisman critical turbulence criterion are necessary but not sufficient conditions for the initiation of phytoplankton blooms (Platt *et al.*, 1991).

The late winter/early spring blooms are primarily governed by irradiance (Legendre, 1990), and given the major role that light plays in photosynthesis, solar radiation seems the best candidate to trigger a physiological activation mechanism at the individual level (Falkowski *et al.*, 1985). At the community level, under any of the hypotheses of bloom development, meteorological conditions are also of primary importance (Ueyama and Monger, 2005). The critical depth hypothesis has solar radiation as a key factor because it controls the euphotic depth (z_{eu}) and thus the PAR regime experienced by phytoplankton, but also the heating of the surface layer which drives the consolidation of thermal stratification that defines the surface MLD. The critical turbulence hypothesis focuses on the turbulence level in the water column, whose principal generating force is wind stress (Backhaus *et al.*, 2003), which can explain as much as the 60% of the variation in the turbulent kinetic energy dissipation rate (MacKenzie and Leggett, 1993). Summing up, meteorological conditions, particularly incident solar radiation and wind stress, appear to be the ultimate factors underlying bloom initiation and

Table I: Cruise day, day of the year and date of sampling of each transect

Year	Transect	Cruise day	Day of the year	Date
2004	R1	1	65	05 Mar
2004	R2	4	68	08 Mar
2004	R3	6	70	10 Mar
2004	R4 ^a	7	71	11 Mar
2004	R5	9	73	13 Mar
2004	R6	12	76	16 Mar
2005	R1	1	54 (420)	23 Feb
2005	R2 ^a	3	56 (422)	25 Feb
2005	R3	7	61 (427)	01 Mar
2005	R4	13	67 (433)	07 Mar
2005	R5	16	70 (436)	10 Mar
2005	R6	19	73 (439)	13 Mar
2005	R7	22	76 (442)	16 Mar
2005	R8	25	79 (445)	19 Mar

^aIndicates transects not sampled completely and, hence, not shown in Figs 4, 6 and 7).

development (Smetacek and Passow, 1990, Ueyama and Monger, 2005).

The objective of this work is to investigate the meteorological and hydrographic factors that drive the initiation of phytoplankton blooms in a temperate ecosystem during late winter/early spring. With this aim, we analysed phytoplankton short-term bloom dynamics in shelf and oceanic waters of the Central Cantabrian Sea (Southern Bay of Biscay) in relation to concurrent meteorological and hydrographical conditions, considering the response of both the pico- and micro-phytoplankton components of the community [<5 and >5 μm equivalent spherical diameter (ESD) respectively].

METHOD

Study site and sampling strategy

Two oceanographic cruises were carried out aboard R/V *García del Cid* in the Central Cantabrian Sea from 5th to 16th March 2004 (DINAPROFIT0304) and from 23rd February to 19th March 2005 (DINAPROFIT0205) (Table I). On the first of these cruises, an across-shelf transect of five oceanographic stations from the coast to the open ocean was sampled six times, whereas on the second cruise, the same transect, enlarged by one station for a better characterization of the variability in the oceanic area, was sampled eight times (Fig. 1 and Table II).

At each station, water column profiling was undertaken using a CTD rosette sampler (Mark-III), a

fluorescence sensor (SeaTech) and Niskin bottles for water sampling at discrete depths for the analysis of nutrients, size-fractionated (0.2–5 and >5 μm size-fractions) chlorophyll *a*, *b* and *c* and pico- and micro-phytoplankton abundance.

Water samples for the measurement of chlorophyll concentration were taken at 3, 20, 40 and 80 m, and collected in dark bottles to avoid pigment damage. For each sample, 100 mL were filtered at low vacuum pressure (<100 mm Hg) sequentially through 0.2 and 5 μm polycarbonate filters (Millipore). Filters were kept frozen for later analysis in the laboratory. Chlorophyll was extracted with 90% acetone for 24 h at 4°C and chlorophyll *a*, *b* and *c* were measured with a spectrofluorometer (Perkin Elmer LB-50s). Total chlorophyll concentration (Chl_T) was calculated as the sum of the three chlorophyll types in both size-fractions. Fluorescence measurements from the rosette fluorometer sensor (*F*) were calibrated against Chl_T [$\text{Chl}_T = (3.2 \pm 0.2) F + (0.16 \pm 0.07)$, $n = 464$, $r^2 = 0.65$; $\text{Chl}_T = (1.8 \pm 0.1) F + (0.02 \pm 0.04)$, $n = 294$, $r^2 = 0.54$ for DINAPROFIT cruises 0304 and 0205, respectively]. Nutrient concentrations (ammonium, nitrite, nitrate, silicate and phosphate) were analyzed by replicated segmented flow analysis with a Skalar San Plus System auto-analyzer (Grashoff *et al.*, 1983). Due to the positive co-variance observed between the nutrients [correlation coefficients for the deseasonalized and detrended nutrient time series from 0 to 100 m for nitrate versus phosphate varies between 0.28 and 0.49 ($P < 0.04$), and for nitrate versus silicate between 0.27 and 0.64 ($P < 0.04$)], only the distribution of nitrate is considered in the present work.

The abundance of phototrophic pico-plankton was determined by flow cytometry (FACSalibur, Becton & Dickinson). Water samples of 1.8 mL were fixed with 1% paraformaldehyde plus 0.05% glutaraldehyde solution, deep-frozen in liquid N_2 and stored at -70°C until analysis. Samples for the analysis of micro-phytoplankton (50 mL) were stored in dark bottles and fixed with 8 mL of lugol solution. Twenty-five millilitre of each sample was settled in Utermöhl chambers (Utermöhl, 1958) and analysed with an inverted microscope to define the species composition during the bloom.

Auxiliary information

Several meteorological data sets were consulted to gather meteorological information. The time series were compared among them and selected on the basis of data quality, resolution and proximity to the sampled transect. Daily time series of atmospheric pressure, air temperature and wind speed recorded at a meteorological station at sea (Cabo Peñas buoy, maintained by

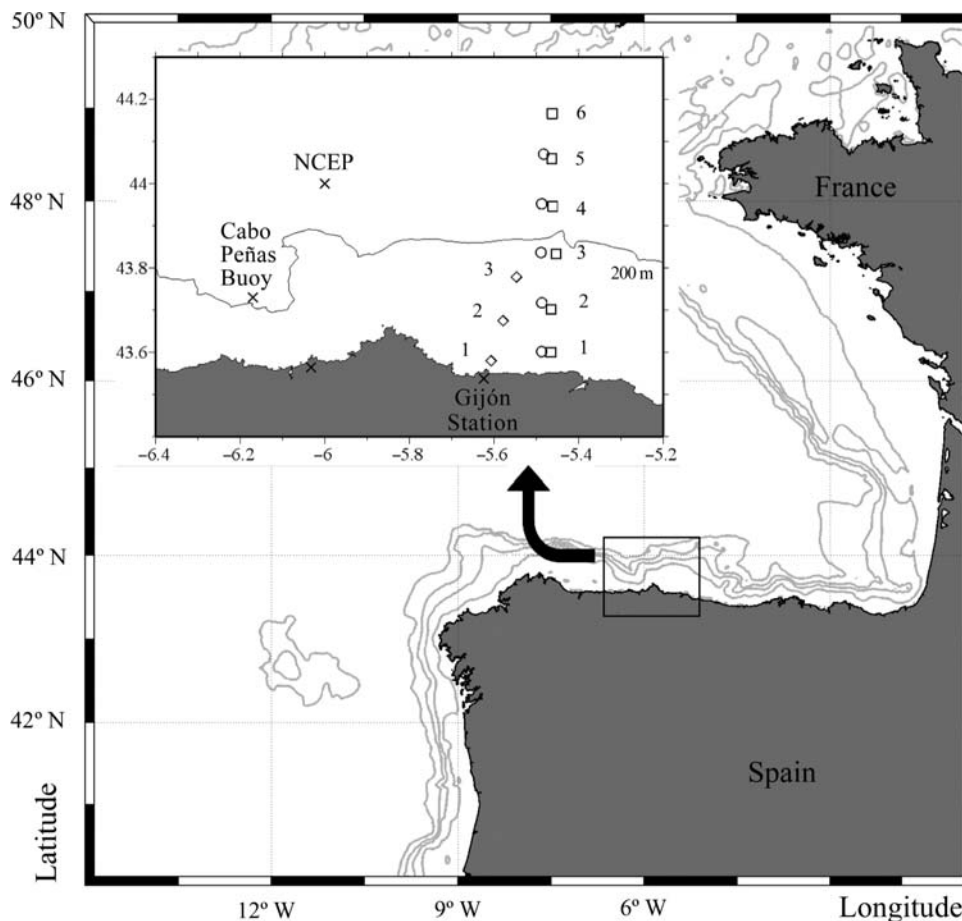


Fig. 1. Map of the study area showing the location of the hydrographic [○ DINAPROFIT0304 (1–5), □ DINAPROFIT0205 (1–6), ◇ Gijón transect from the RADIALES monitoring programme (1–3)] and meteorological stations (×).

Puertos del Estado from the Ministerio de Fomento, http://www.puertos.es/es/oceanografia_y_meteorologia, Fig. 1) for the period February–March 2004 and 2005 were analysed to define the meteorological scenario experienced during the cruises. Solar radiation data were obtained from the *NCEP/NCAR Reanalysis* dataset (<http://www.cdc.noaa.gov/data/gridded/data.ncep.reanalysis.html>) provided by the National Oceanic & Atmospheric Administration (NOAA) for 2004, and from the meteorological station on land for 2005 [Gijón

station, checked and approved by the Agencia Estatal de Meteorología (AEM) from Ministerio de Medio Ambiente y Medio Rural y Marino, <http://www.ronzon.com>, Fig. 1]. Solar radiation data from Gijón station and from NCEP for 2005 were compared (correlation coefficient 0.68) indicating that 2004 data from the NCEP could be used with reliability.

Oceanographic data from the scientific time-series monitoring programme RADIALES (<http://www.seriestemporales-ieo.net/>) were also used to define the seasonal context. The time series of monthly data from 2001 to 2005 collected at the Gijón section, which is partly coincident with the sections sampled during the DINAPROFIT cruises (Fig. 1), were used to explore the correlation between physical and biogeochemical variables. The seasonality of the years 2004 and 2005 represented in Fig. 2 was derived from the same data. Variables measured and sampling protocols applied in the Gijón section were similar to those used during the DINAPROFIT cruises and can be consulted elsewhere (e.g. Calvo-Díaz *et al.*, 2008).

Table II: Location and depth of each sampling station.

Station	Latitude (°N)	Longitude (°W)	Distance to coast (NM)	Depth (m)
1	43.600	−5.465	0.3	80
2	43.701	−5.465	7.1	145
3	43.833	−5.453	13.9	160
4	43.946	−5.461	20.7	750
5	44.059	−5.463	27.5	1800
6	44.166	−5.462	33.3	3400

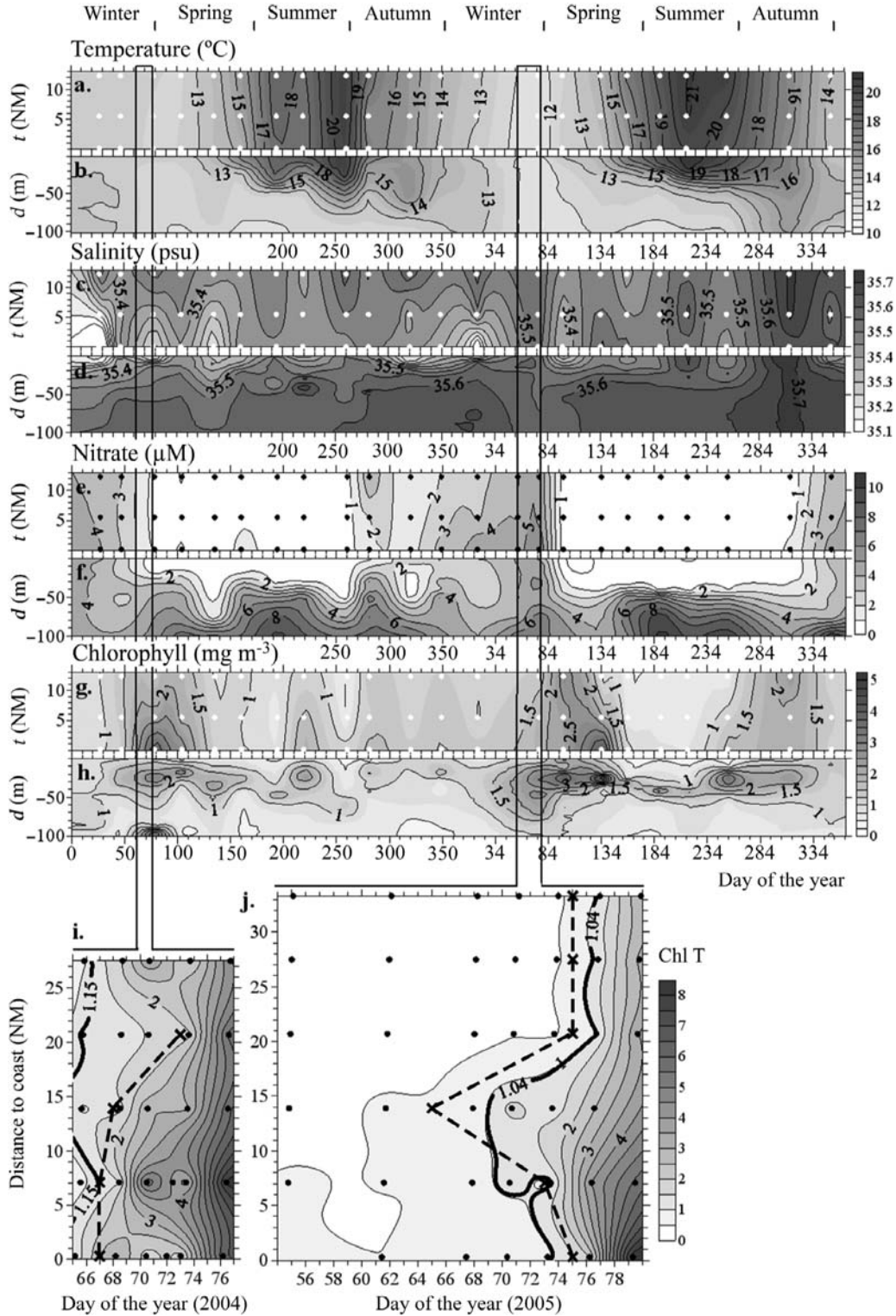


Fig. 2. Seasonal variation of the physical and biogeochemical environment in 2004 and 2005 derived from the monthly time series monitoring programme RADIALES, and short-term variation of total chlorophyll during the DINAPROFIT cruises. Temporal variation of the surface fields [across-shelf distance (t (NM)) versus time] and water column profiles at the mid-shelf [depth (d (m)) versus time at stn. 2 in the Gijón section] of: (A and B) temperature ($^{\circ}\text{C}$), (C and D) salinity (psu), (E and F) nitrate (μM) and (G and H) Chl_T (mg m^{-3}). (I and J) Time course of surface (above 25 m depth) Chl_T (mg m^{-3}) during the cruise carried out in 2004 and 2005; thick black lines indicate bloom onset following Siegel's criterion (Siegel *et al.*, 2002) and dotted-line indicate bloom onset derived from the break-points of the split linear regression model fitted to Chl_T time series (Table V).

Table III: Means of atmospheric pressure (P , mb), air temperature (T_a , °C), solar radiation (R , $W\ m^{-2}\ h^{-1}$) and wind speed (W , $m\ s^{-1}$) for the reference period and for each meteorological scenario established on the basis of variations in solar radiation and wind speed and experienced during the 2004 and 2005 cruises.

		Scenario		
Reference mean		1	2	3
Means for reference period				
2004				
P	1019.3	1010.1	1022.6	1027.4
T_a	10.2	8.3	10.4	12.3
W	5.9	7.8	5.7	4.0
R	149.3	132.4	143.4	188.5
2005				
P	1019.8	1014.1	1026.7	1017.6
T_a	10.2	6.8	8.3	12.2
W	5.8	7.8	8.7	4.2
R	119.8	93.3	199.3	167.3

Data analysis

The cumulative sums method (Ibanez *et al.*, 1993) was applied to the meteorological time series to determine the dates, intensity and duration of the major changes of the meteorological conditions. The method permits

the definition of homogeneous time intervals in the series relative to a reference period:

$$S_p = \sum_{i=1}^p x_i - pk \tag{1}$$

where, S_p is the cumulated function; x_i , the value i of variable x in the time series; p , the number of data points and k the mean value for the reference period. Three meteorological scenarios were defined on the basis of changes observed in solar radiation and wind speed. The local means (averages for each homogeneous time interval or scenario, Table III), which are defined by the slope of the cumulative function (Fig. 3), were compared among them and with the reference means (February–March of 2004 and 2005, respectively) using a paired t -Student test (Table IV) to assess the significance level of the observed changes.

The temporal variation of the across-shelf distribution of physical (temperature and salinity profiles from the CTD), biogeochemical variables (Chl_T from fluorescence values and nitrate and chlorophyll a , b and c from water samples at discrete depths) and ratios between phytoplankton size-fractions was illustrated as contour images. Contouring was made using SURFER 8.0 (© Golden Software, Inc.) with Krigging as the interpolation method.

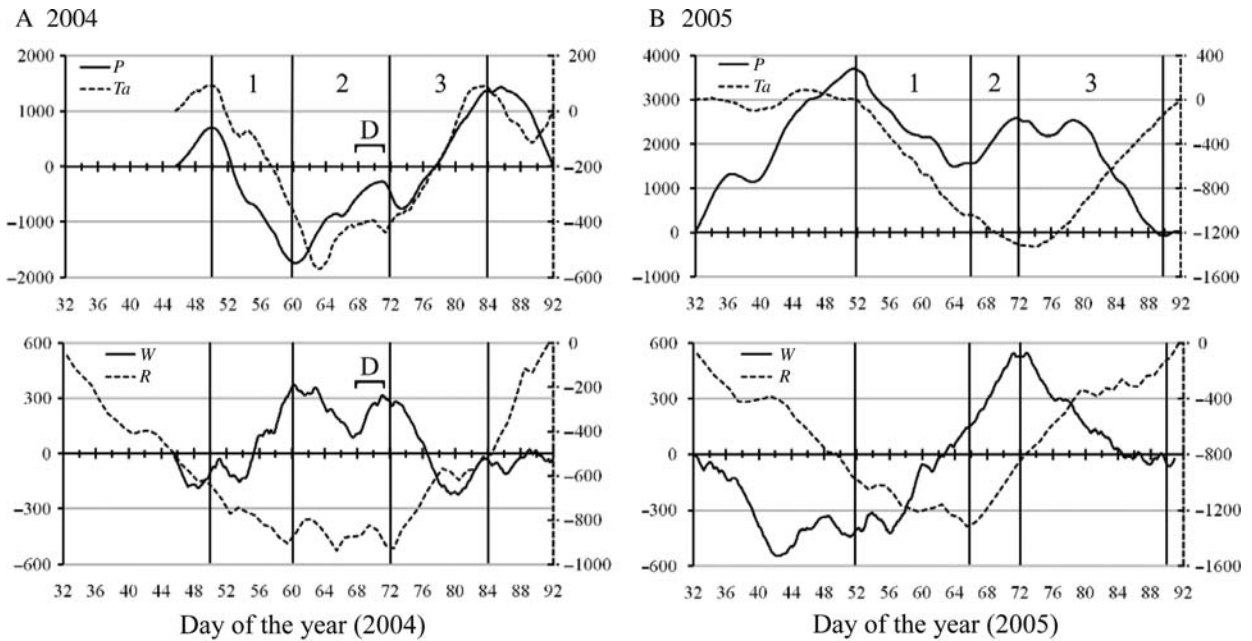


Fig. 3. Time series of the cumulative sums of atmospheric pressure (P , mb, left axis), air temperature (T_a , °C, right axis), solar radiation (R , $W\ m^{-2}\ h^{-1}$, left axis) and wind-speed (W , $m\ s^{-1}$, right axis) during February–March of (A) 2004 and (B) 2005 used to define the meteorological scenarios (inserted numbers) experienced during the cruises (Table III). In 2004, the occurrence of a meteorological disturbance is also noted (D).

Table IV Comparison between reference means (Ref. mean) and means for consecutive meteorological scenarios of atmospheric pressure (P), air temperature (T_a), solar radiation (R) and wind speed (W) by means of a paired t -Student test.

	2004				2005			
	P (mb)	Ta (°C)	R (W m ⁻² s ⁻¹)	W (m s ⁻¹)	P (mb)	Ta (°C)	R (W m ⁻² s ⁻¹)	W (m s ⁻¹)
Ref. mean vs Scenario 1	*	*	**	**	*	*	**	*
Ref. mean vs Scenario 2						*	*	*
Ref. mean vs Scenario 3	*	*	*		*	*	*	*
Scenario 1 vs Scenario 2	*	*		**	*	*	*	*
Scenario 2 vs Scenario 3	*	*	*	*	*	*	*	*
Scenario 2 vs Scenario 3		*	*		*	*	*	*

* $P < 0.05$.

** $P < 0.1$.

Temperature- and density-based criteria were used to define the MLD. MLD was calculated as the depth where temperature is 0.5 (Levitus, 1982) and 0.2°C (Thompson, 1976) below surface temperature, respectively, and as the depth where density is 0.125 kg m⁻³ below surface density (Levitus, 1982).

The onset of the bloom was calculated following Siegel's criterion (Siegel *et al.*, 2002), which calculates the day of the bloom onset as the day when Chl level first rises a 5% threshold above annual median values. Annual chlorophyll data were obtained from station 2 of the Gijon section from the monthly time-series monitoring programme RADIALES.

Nitrate and chlorophyll data averaged for the surface layer of the water column (between 3 and 25 m) for all sampling stations were analysed to determine significant temporal changes (Table V). Due to the short-length of these time series, they were characterized using a split-linear regression model in order to define the dates and rates of significant changes in the time series:

$$y_1 = a_1 + b_1x \quad (2)$$

$$y(x_0) = a_1 + b_1x_0. \quad (3)$$

$$y_2 = y(x_0) + b_2(x - x_0) \quad (4)$$

where, a_1 and b_1 are, respectively, the intercept and slope coefficients of the first linear regression; $y(x_0)$ and b_2 are the intercept and slope coefficients of the second linear regression; and $(x_0, y(x_0))$ is the point where both lines converge (or break-point of the split-linear regression). For the 2004 time series, in order to take into account the effect of the meteorological disturbance that occurred during the cruise, the split linear regression model was fitted to two nitrate and chlorophyll data sets (Table V); the first one [2004(1)] integrated for all the data previous to the disturbance, and the second one [2004(2)] integrated for all the data except those corresponding to the first increase in chlorophyll. The software used to carry out the split-linear regressions was GRAPHPAD PRISM 4.0 (© GraphPad Software, Inc.).

RESULTS

Seasonal variation in 2004 and 2005

The seasonal processes of surface warming and progression of the seasonal thermocline typical of a

Table V: Parameters of the split-linear regression models fitted to Chl_T and nitrate values for 2004, before [2004(1)] and after the meteorological disturbance [2004(2)], and 2005 (Fig. 5)

	2004 (1)		2004 (2)		2005	
	Nitrate	Chlorophyll T	Nitrate	Chlorophyll T	Nitrate	Chlorophyll T
x_0	66.4 ± 0.9	67 ± 2	73.0 ± 0.5	72.2 ± 0.5	71 ± 2	74.5 ± 0.7
b_1	0.10 ± 0.03	0.01 ± 0.02	0.08 ± 0.02	0.01 ± 0.01	0.15 ± 0.03	-0.00 ± 0.01
b_2	-1.19 ± 0.27	0.45 ± 0.09	-1.37 ± 0.22	1.24 ± 0.16	-0.65 ± 0.23	0.92 ± 0.18
n	24	33	36	21	45	43
R^2	0.70	0.64	0.68	0.90	0.50	0.70

temperate shelf sea (Longhurst, 1998) can be seen in Fig. 2A–B. The seasonal thermocline developed around March–April (around days 120 and 84, in 2004 and 2005, respectively), becoming progressively deeper and stronger up to August (days 250 and 234). From September, the thermocline started to be eroded due to surface cooling and wind-driven mixing associated with the passage of atmospheric low pressure systems. A weak stratification could still persist until November–December, when the thermocline definitely broke down (around days 365 and 334). The processes of seasonal stratification/de-stratification occurred, respectively, earlier/later in the oceanic than in the coastal domain (Fig. 2A).

The annual variation of the distribution of salinity is mainly controlled by freshwater runoff, which tends to occur during winter and early spring as short-lived pulses. The monitoring programme detected three of them in 2004 (between days 1 and 120) and only one in 2005 (around day 10), which generated steep across-shelf [$0.3–0.6$ psu per nautical mile (NM^{-1}); Fig. 2C] and vertical gradients (halocline at 15–25 depth, $\Delta S = 6 \cdot 10^{-3}$ psu m^{-1} ; Fig. 2D). Offshore, high salinity values (>35 psu) were measured in summer, concurrent with maximum surface thermal stratification (on days 260 and 234), and between September and March, when the incursion of the Iberian Poleward Current (IPC) into the Northern Iberian margin has its maximum expression (development phase of the IPC) (Peliz *et al.*, 2005).

Nutrients exhibit marked seasonality. For example, the distribution of nitrate in 2004 and 2005 showed two well-defined periods (Fig. 2E and F). During spring-summer, oligotrophic conditions ($<1 \mu\text{M}$) prevailed in the surface layer (nutricline between 10 and 40 m depth) concurrent with thermal stratification (Fig. 2A and B) (days 120–270 and 84–300). The rest of the year, nitrate was well mixed and concentrations were higher than $4 \mu\text{M}$. Maximum values ($>8 \mu\text{M}$) occurred at the bottom in summer (around day 200 in 2004; between days 170 and 270 in 2005), presumably linked to coastal upwelling and remineralization on the bottom shelf. There is a negative correlation between the deseasonalized and detrended temperature and nitrate concentration time series [correlation coefficient at 75 m = -0.66 ($P < 0.000$)].

At the annual scale and from monthly data, the distribution of chlorophyll (Chl_T) in 2004 and 2005 showed some similarities (Fig. 2G and H). The spring bloom occurred around March ($\text{Chl}_T > 2 \text{ mg m}^{-3}$; around days 60 and 84), and relative high values lasted for 1–2 months (two to three consecutive sampled dates) and extended all along the section from coastal to mid-shelf waters (Fig. 2G and H). However, it must be

noticed that at higher resolution the dynamics of the spring bloom (discussed below) look quite different (Fig. 2I and J) in terms of onset day, rate of biomass increase and persistence. The highest values during the spring bloom were measured near the surface (<20 m depth). From late-spring to summer, concurrent with the stratified, oligotrophic phase, surface chlorophyll decreased below 1 mg m^{-3} , more acutely in 2005 than in 2004, and a subsurface maximum developed near the nutricline (Fig. 2F). A secondary bloom was detected in summer 2004 (day 220), apparently linked to coastal upwelling according to the uplift of isotherms (Fig. 2B) and enhanced concentration of nitrate near the bottom layer (Fig. 2F). An autumn bloom was detected in October 2005 (around day 300), during the phase of erosion of the seasonal thermocline. There is a positive correlation between the deseasonalized and detrended nitrate and chlorophyll time series [correlation coefficient at 10 m = 0.35 ($P = 0.05$)].

Meteorological scenario February–March 2004 and 2005

2004 (February 15th to March 31st)

Before the cruise, between days 50 and 60 (scenario 1), the meteorological variables defined a situation of relatively bad weather, characterized by lower-than-average values of atmospheric pressure, air temperature and solar radiation (local means: $P = 1010.1$ mb, $T_a = 8.3^\circ\text{C}$ and $R = 132.4 \text{ W m}^{-2} \text{ h}^{-1}$, respectively) and higher-than-average wind-speed ($W = 7.8 \text{ m s}^{-1}$) (Fig. 3A and Table III). From days 60 up to 72 (scenario 2), thus covering the initial part of the cruise (Table I), the weather improved as indicated by the increase in P , T_a and R (1022.6 mb, 10.4°C , $143.4 \text{ W m}^{-2} \text{ h}^{-1}$) and the decrease in W (5.7 m s^{-1}). The local mean of R during this time interval was not significantly different from the reference mean, while W was significantly lower (Table IV). However, a short-term meteorological disturbance caused by the passage of a low pressure system induced a sharp increase of W (12 m s^{-1}) between days 68 and 72. During the last days of the cruise, from day 73 onwards (scenario 3), a further improvement in the weather occurred: T_a and R were significantly higher-than-average (1027.4 mb, 12.3°C , $188.5 \text{ W m}^{-2} \text{ h}^{-1}$) and W was significantly lower-than-average (4.4 m s^{-1}), although not significantly different from the previous scenario (Table IV).

2005 (February 1st to March 31st)

A scenario of relatively bad weather, lower-than average P , T_a and R (1014.1 mb, 6.8°C , $93.3 \text{ W m}^{-2} \text{ h}^{-1}$) and

higher-than average W (7.8 m s^{-1}), occurred from day 52, some days before the start of the cruise (on day 54), up to day 66 (scenario 1) (Fig. 3B and Table III). From day 66 onwards (scenario 2), due to a high pressure centre over the North Atlantic, P , T_a and R increased significantly (1026.7 mb , 8.3°C , $199.3 \text{ W m}^{-2} \text{ h}^{-1}$), while W remained higher-than the average (8.7 m s^{-1}). The change of W from day 72 onwards (scenario 3) defined the scenario of the last days of the cruise: P , T_a and R maintained the relatively high levels of the previous scenario, while W descended significantly (4.2 m s^{-1}) (Table IV).

Hydrographic conditions during the cruises

2004 (March 5th to 16th)

During the first days of the cruise (days 65–68), the vertical distribution of isoclines of temperature and salinity indicate almost complete mixing (Fig. 4A). The across-shelf distribution showed a clear gradient from fresher and cooler coastal waters to saltier and warmer oceanic waters. A weak front at ca. 18 nautical miles offshore (station 4) separated both domains. The front

strengthened on day 70 when a lens of fresh and cool water extended from the coast up to the frontal area. The last days of the cruise (days 73 and 76), concurrent with the improvement of the weather (third meteorological scenario), thermal stratification developed, progressing from the oceanic to the coastal domain. The thermocline became shallower and stronger at the end of the cruise. At station 3, for instance, the MLD was at 150 m depth from days 65 to 73, shoaling to 19 m according to the 0.5°C bulk temperature difference criterion or to 42 m according to the 0.125 kg m^{-3} bulk density difference criterion 5 days later (78) (Fig. 5A) [or to 18 m 3 days later (76) with the 0.2°C criterion].

The distribution of nitrate remained relatively homogeneous ($>4 \mu\text{M}$) during most of the cruise (days 65–73). The main characteristics were the relatively lower concentrations at the surface ($2\text{--}3 \mu\text{M}$), and higher ($<5 \mu\text{M}$) at the coast and at the mid-shelf front (day 70) (Fig. 4A). A more detailed analysis indicated that nitrate concentration in the surface layer ($<25 \text{ m}$ depth) showed a saw-tooth pattern: it decreased from day 66, increased on day 70

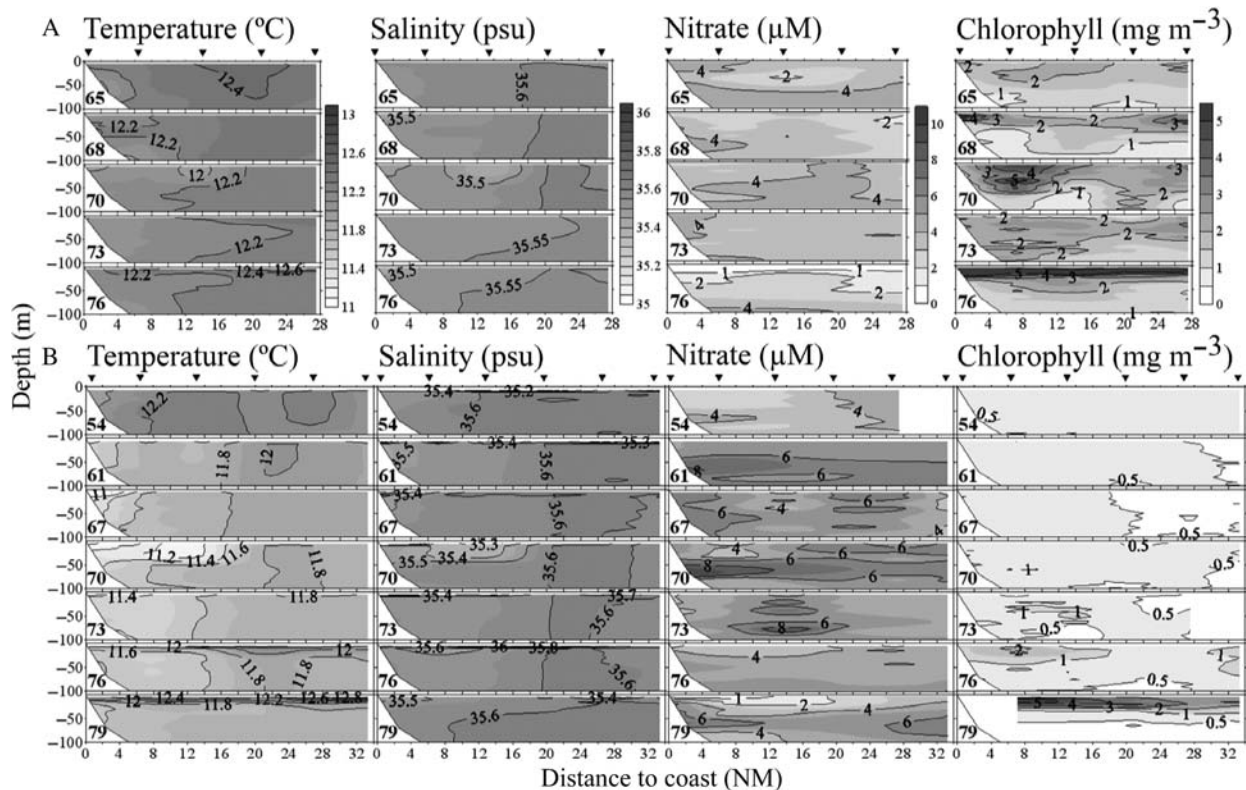


Fig. 4. Temporal evolution of the across-shelf distribution of temperature ($^\circ\text{C}$), salinity (psu), nitrate (μM) and total chlorophyll (mg m^{-3}) during the cruises carried out in (A) 2004 and (B) 2005. The day of the year is indicated in the lower left hand corner of each panel and the locations of the sampling stations are indicated along the top of the figure (∇).

concurrent with a meteorological disturbance, and decreased again from day 73 onwards (Fig. 5B and Table V). The last day of the cruise the surface concentration dropped below $1 \mu\text{M}$ and a nutricline developed at around 10 m depth (Fig. 4A).

Total chlorophyll remained at relatively high concentrations (around 2 mg m^{-3}) at the surface (above 30 m depth) during most of the cruise. Patches of high chlorophyll concentration ($3-4 \text{ mg m}^{-3}$) were found at the coastal and oceanic stations (days 65 to 70). On the last day of the cruise, the concentration in the surface layer increased to $>4 \text{ mg m}^{-3}$. Nitrate and chlorophyll fields co-varied negatively, especially where patches of high chlorophyll were detected (e.g. $\text{Chl}_T >4 \text{ mg m}^{-3}$ at the oceanic station on day 68) and when the bloom was well underway (day 76) (Fig. 4A).

2005 (February 23rd to March 19th)

The hydrographic conditions during the first 10 days of the cruise resemble those observed in the previous year (Fig. 4B): complete vertical mixing, a steep across-shelf gradient and a mid-shelf front were observed. An

intense freshwater runoff pulse on day 67 enhanced the across-shelf gradient and strengthened the frontal structure that separates the fresher and cooler (note the strong thermal inversion on day 70) coastal side of the front from the saltier and warmer oceanic side. During the last days of the cruise (days 76-78), thermal stratification developed throughout the section, and a clear thermocline formed at around 20 m depth (Fig. 4B). At station 3, for example, the MLD was at 150 m depth from days 54 to 73, shoaling to 6 m 3 days later (76) according to the 0.5°C bulk temperature difference criterion (Fig. 5B) and the 0.2°C criterion or to 40 m 6 days later according to the 0.125 kg m^{-3} bulk density difference criterion (Fig. 5B).

Nitrate and chlorophyll showed an almost homogeneous distribution, with values $>6 \mu\text{M}$ and $<0.5 \text{ mg m}^{-3}$, respectively, during most of the cruise. Chlorophyll increased ($>2 \text{ mg m}^{-3}$) and nitrate decreased ($<2 \mu\text{M}$) in the surface layer towards the end of the cruise (Fig. 4B). Nutrient time series showed that surface nitrate decreased significantly from day 70 (Fig. 5B and Table V).

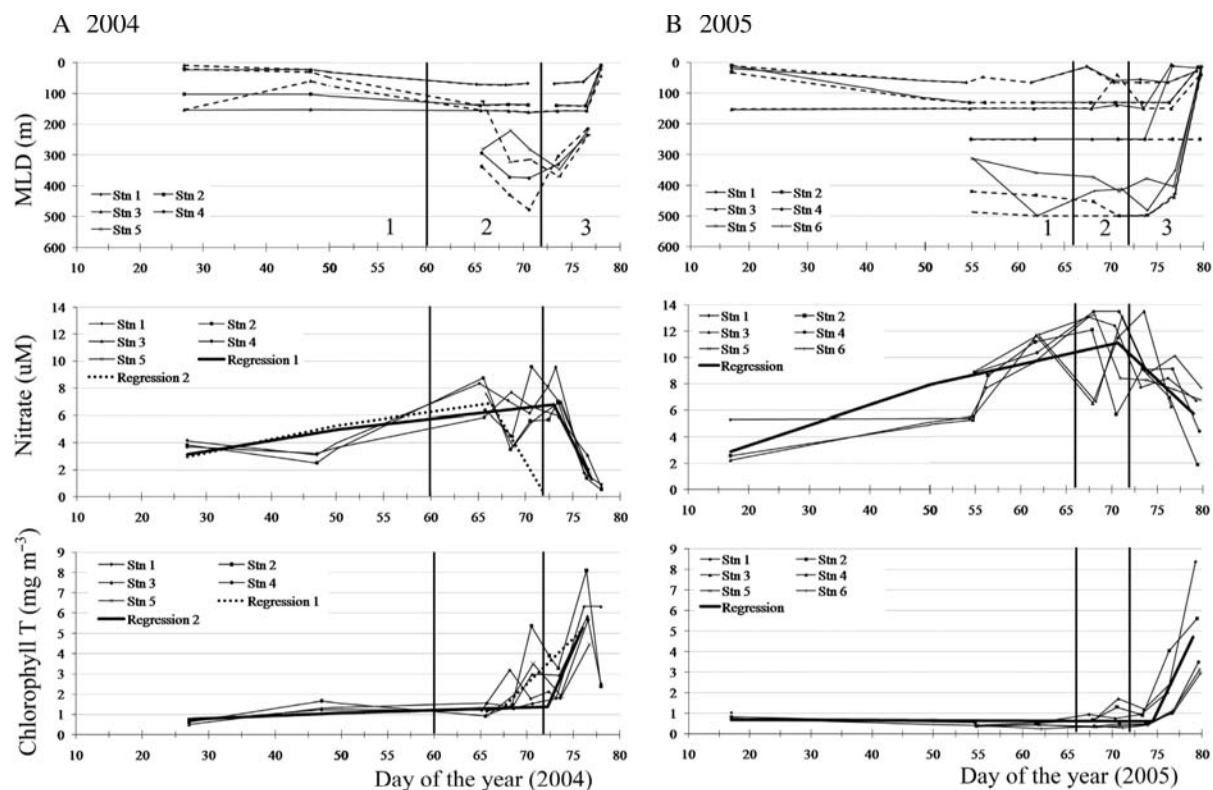


Fig. 5. Time series of mixing layer depth (MLD) according to the 0.5°C temperature difference (solid line) and to the 0.125 kg m^{-3} density difference (dashed line), nitrate (μM) and Chl_T (mg m^{-3}) for each sampling station during (A) the cruises of 2004, and (B) 2005. Surface nitrate and surface chlorophyll concentration were analysed by means of a split-linear regression model to find significant points of change (Table V). Note that time scale is compressed for the first 50 days. Meteorological scenarios are also indicated (inserted numbers).

Phytoplankton dynamics

2004 (March 5th to 16th)

Following Siegel's criterion (Siegel *et al.*, 2002), the onset of the bloom ($\text{Chl}_T > 1.2 \text{ mg m}^{-3}$) occurred around day 65 (March 5th) (Fig. 2I), while according to the breakpoint criterion it occurred around day 67 ($n = 33$, $r^2 = 0.64$). The phytoplankton biomass baseline prior to the bloom had a slope not significantly different from zero, whereas after the onset of the bloom the slope increased significantly (Table V). However, around day 68, chlorophyll concentration decreased concurrently with an increase in wind speed associated with the passage of a meteorological disturbance (Fig. 3A). After the disturbance, the accumulation of biomass resumed (day 72). The chlorophyll maximum was reached at the end of the cruise, on day 76 (March 16th) (Fig. 5A). The major contribution to the bloom was due to organisms larger than $5 \mu\text{m}$. Before the onset, the ratio between small- and large-sized phytoplankton was >1 , whereas after the onset it changed to <1 throughout the across-shelf section (Fig. 6A).

The bloom began first at stations 2, 3 and 5 and with some delay at stations 1 and 4. Chlorophyll

concentration at stations 2, 3 and 5 was also high at the sub-surface ($>2 \text{ mg m}^{-3}$ below 25 m depth), while it was highest at the surface at stations 1 and 4, where concentrations below 25 m depth were $<0.5 \text{ mg m}^{-3}$ (Fig. 7). The maximum chlorophyll *a* in the large-sized fraction was 4 mg m^{-3} . Chlorophyll *c* showed the same variation pattern as chlorophyll *a*, with maximum concentrations of 1 mg m^{-3} . Chlorophyll *b* content in this size fraction was negligible (Fig. 7). The bloom was dominated by *Guinardia* sp., and to a lesser extent by *Rhizosolenia* sp. and *Meuneria* sp.

Variations in the smaller size fraction were subtle but obvious. The higher chlorophyll *a* concentrations (0.4 mg m^{-3}) were observed at the end of the cruise at the oceanic stations (stations 4 and 5). Chlorophyll *b* followed the same pattern, with concentrations around 0.2 mg m^{-3} at the end of the cruise at the oceanic stations. Size fraction $<5 \mu\text{m}$ lacks, almost completely, chlorophyll *c* (Fig. 7). *Prochlorococcus* was absent, while *Synechococcus* and pico-eukaryotes were limited to the oceanic area.

2005 (February 23rd to March 19th)

The onset of the bloom in 2005 occurred on day 73 (March 13th) according to the Siegel's criterion (Chl_T

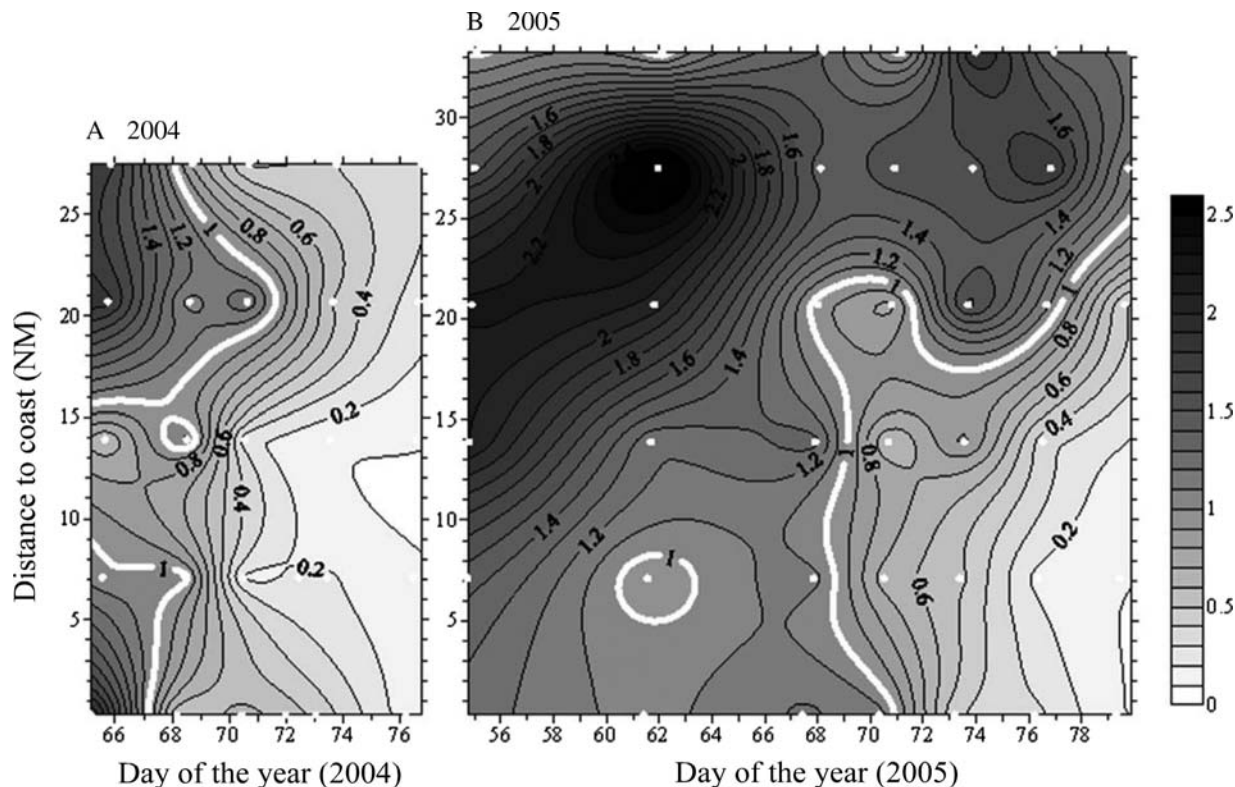


Fig. 6. Time course of the across-shelf ratio between the biomasses (Chl_T as a proxy) in the <5 and $>5 \mu\text{m}$ ESD size-fractions during the cruises of (A) 2004 and (B) 2005. White lines indicate ratio = 1.

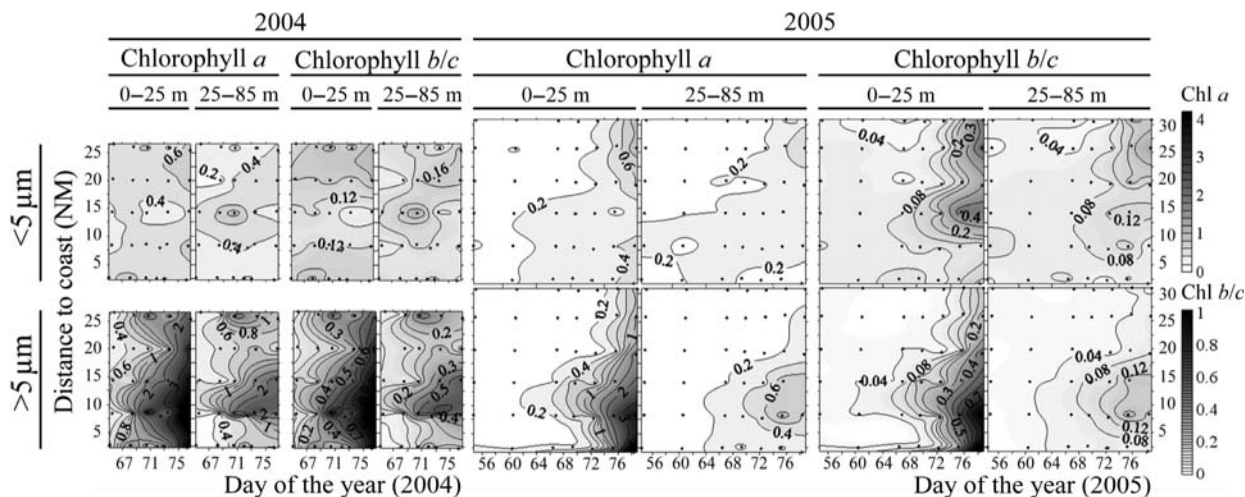


Fig. 7. Time course of the across-shelf distribution of surface (above 25 m depth) and sub-surface (between 25 and 85 m depth) chlorophyll concentration during the cruises of 2004 and 2005 in the $<5 \mu\text{m}$ ESD (chlorophyll *a* and *b*) and in the $>5 \mu\text{m}$ ESD size-fractions (chlorophyll *a* and *c*).

$>1.04 \text{ mg m}^{-3}$ (Fig. 2J) and on day 74 according to the breakpoint of the split-linear regression ($n = 43$, $r^2 = 0.70$) (Table V). Biomass baseline prior to the bloom had a slope not significantly different from zero while wind speed maintained high values, whereas after the onset of the bloom the slope increased significantly concurrently with the amelioration of the meteorological conditions. The maximum chlorophyll maximum was reached on day 79 (March 19th) (Fig. 5B).

The major contribution to the bloom was due to organisms larger than $5 \mu\text{m}$ in the coastal and shelf area, when the ratio between small- and large-sized was >1 before the onset of the bloom and shifted to <1 afterwards. Contrasting with the situation observed in 2004, in the oceanic area the bloom was dominated in terms of biomass by organisms in the smaller size-fraction, and consequently the ratio remained <1 (Fig. 6B).

The bloom began in the shelf area (stations 2 and 3) and at the coastal and oceanic stations (4, 5 and 6) later on. At the oceanic stations, chlorophyll *a* increased in the surface (1 mg m^{-3}), while at the shelf stations the concentrations were also higher ($>1 \text{ mg m}^{-3}$) in the sub-surface layer (below 25 m depth) (Fig. 7). Chlorophyll *c* followed a similar pattern but with lower concentrations (maximum 1 mg m^{-3} in stations 1 and 2). At the coastal stations *Chaetoceros* sp., *Pseudonitzschia* sp. and *Rhizosolenia* sp. dominated the phytoplankton community, whereas at the oceanic stations the more abundant groups of micro-phytoplankton were dinoflagellates (*Ceratium* sp. and *Peridinium* sp.) and to a lesser extent diatoms such as *Pseudonitzschia* sp. and *Thalassionema* sp.

The smaller size-fraction dominated at the oceanic stations (5 and 6), where it reached values around

1 mg m^{-3} at the end of the cruise; coastal values did not exceed 0.4 mg m^{-3} . Chlorophyll *b* concentration was relatively high (maximum 0.5 mg m^{-3}); it began to increase in station 3 at the same time of the bloom, but only in the surface. At the oceanic stations, the increase was lagged and took place also in the sub-surface layer (Fig. 7). *Prochlorococcus* was observed on the last days of February, but it disappeared towards the end of the cruise. *Synechococcus* and pico-eukaryotes, homogeneously distributed at the beginning of the cruise, increased their abundance at the oceanic stations during the bloom.

DISCUSSION

Seasonality and phytoplankton

Phytoplankton communities seem to have little buffering capacity against environmental changes, which imply that the dynamics of phytoplankton population is under tight bottom-up environmental control (Smayda, 1998). This fact becomes apparent in the annual data from the long-term monitoring programme RADIALES for the years 2004 and 2005 presented here, where physical (temperature, salinity) and biogeochemical variables (nitrate, chlorophyll) covary significantly (Fig. 2). However, it is necessary to be careful with the interpretation of the seasonality deduced from the analysis of monthly data, especially for those variables that show high variability at time scales shorter than the sampling interval. This issue is exemplified by chlorophyll: while its variability deduced from monthly data (Fig. 2G and H) suggests that the short-term, high-resolution cruises

of 2004 and 2005 were carried out when the spring bloom had already begun, data from the cruises (Fig. 2I and J) show that the observed blooms began later and more abruptly. Consequently, a monthly monitoring programme is not capable of capturing the actual characteristics (e.g. timing, intensity and persistence) of these transient events. Nevertheless, a long-term, monthly resolution time series monitoring programme is useful to provide a framework for the interpretation of data with higher resolution. For instance, in the case presented here, the setting of the situation prior to the bloom is important not only to determine temporal evolution or timing of the bloom but also to understand its across-shelf variation.

In 2005, the chlorophyll concentration prior to the bloom was very low, whereas in 2004, the concentration was higher, although steady. Freshwater discharges during the winter in 2004 could have promoted the occurrence of transient freshwater coastal blooms (Legendre, 1990) that, as the freshwater lens moved offshore, caused the relatively high chlorophyll concentration observed all along the section. Thus, the chlorophyll concentration baseline in 2004 was higher than in 2005, which means that local conditions for each year must be taken into account to explain the temporal evolution of the bloom.

The criterion from Siegel *et al.* (Siegel *et al.*, 2002) for bloom onset defines a statistically based chlorophyll *a* threshold which is different for each zone and year (Henson *et al.*, 2006), hence taking into account its spatial and inter-annual variability. However, intra-annual variability is high and Siegel's criterion (Siegel *et al.*, 2002) does not consider the biomass concentration baseline before the bloom. Thus, the method used here based on the adjustment of a split-linear regression model to the biomass values in order to obtain a date for bloom onset takes into account local conditions, showing for instance that biomass concentration is almost steady prior to the bloom, although it may be relatively high as occurred in 2004, whereas after the bloom onset it increases abruptly. This change in biomass does not tell us anything about what is happening with phytoplankton production because we lack data to assess the relative importance of other processes (such as grazing and sedimentation), but it is an evidence of the imbalance between gain and loss terms of biomass (Legendre, 1990).

The blooms observed in 2004 and 2005 began later at oceanic than at coastal stations. Moreover, there were differences in the across-shelf distribution concerning the population of phytoplankton that caused the bloom. Even when both size-fractions responded to bloom conditions, they do it differently in the coastal and oceanic

domains. Most of the year, phytoplankton biomass is dominated by small phytoplankton, while during the annual biomass maxima larger phytoplankton becomes dominant (Tilstone *et al.*, 2003; Calvo-Diaz *et al.*, 2008). In the late-winter blooms reported here, both size-fractions increased their biomass during the bloom but the relative importance of the larger size-fraction, mainly chain forming diatoms, was higher at the coast and inner shelf whereas the relative importance of the smaller size fraction increases in the outer shelf and oceanic area, markedly in 2005.

Both years, a mid-shelf frontal area was observed according to the temperature and salinity across-shelf fields (Fig. 4). This kind of front has been previously reported in the same area and month (Fernández and Bode, 1991) and can be also observed on an annual scale (Fig. 2C). In 2005, the front persisted after the onset of the bloom, which can explain the clear difference in the coastal and oceanic blooms concerning the relative importance of the small- and large-sized phytoplankton components and species composition. In 2004, the mid-shelf front disappeared before the onset of the bloom, giving rise to the relatively homogeneous across-shelf phytoplankton composition observed this year. The differences in the across-shelf distribution of phytoplankton are relevant to the fate of biomass produced during the bloom. In the coastal area, where large-sized phytoplankton tends to dominate, the fate of the phytoplankton biomass will be sedimentation in absence of grazing, whereas in the oceanic area, sedimentation will not be as important giving the amount of biomass allocated to the small-sized phytoplankton which has almost neutral buoyancy. Alternatively, if there is a coupling between primary producers and consumers, in the coastal area the diatoms will be the base of a classical food web whereas in the oceanic area the pico-plankton will support the microbial loop (Azam *et al.*, 1983).

Short-term dynamics: conceptual model of bloom dynamics

To describe the timing of the bloom, it is necessary to focus on two different aspects of bloom development, enhanced primary production and biomass accumulation, each one with their own forcing variables. Bloom timing for both years showed time delays between changes in the expected forcing variables (solar radiation and wind speed) and the phytoplankton response. So, events leading to a bloom can be divided in two periods according to the temporal evolution of phytoplankton in response to external forcing (Fig. 8).

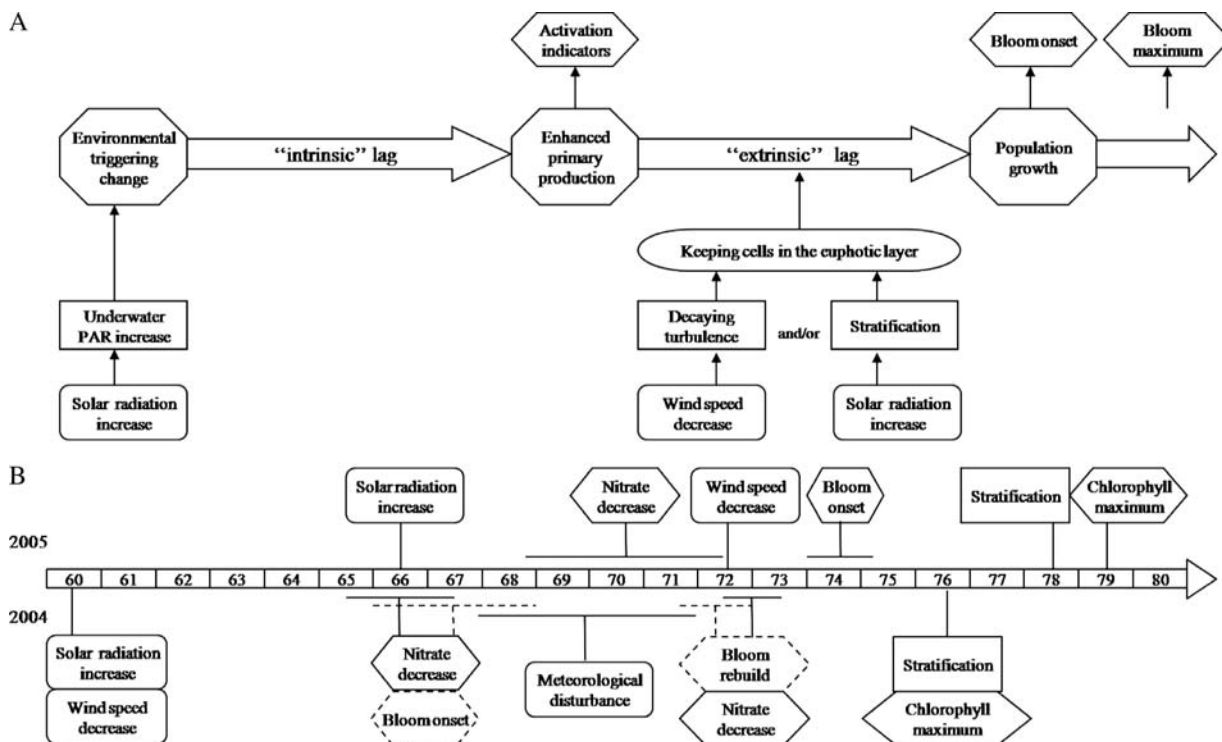


Fig. 8. Conceptual model showing possible timing of late-winter and spring blooms as the combination of two phases, one of physiological adaptation driven by the increase in solar radiation resulting in an enhanced primary production and another one of growth driven by the stability of the water column resulting in biomass accumulation. **(A)** On the basis of the Duarte’s model (octagons) (Duarte, 1990), forcing variables (rounded rectangles), the effect on the water column (rectangles) and the ecosystem response (hexagons) are shown. **(B)** Sequence of events over a time scale (julian day) for 2005 (top) and 2004 (down). Horizontal lines linked to boxes indicate estimated timing errors (Table V).

Time lags between stimuli and algal growth have been previously reported in natural oceanic communities (Duarte, 1990). They can be divided into an “intrinsic” component, that comprises the time lag in the transfer of an environmental triggering factor to enhanced cell division, or primary production in Legendre’s definition (Legendre, 1990), and an “extrinsic” component that represents the delay in the transfer of enhanced cell division to population growth or biomass accumulation (Fig. 8A).

For the intrinsic component, the external forcing variable that seems the best candidate to cause a physiological adaptation under light-controlled conditions, such as those encountered in late-winter and early-spring, is solar radiation as the primary factor that controls underwater PAR. This first lag ends when phytoplankton cells are able to respond to favourable conditions because their metabolic state has adapted (Fig. 8A). In the present work, we have not taken into account any physiologically related variable as an indicator of physiological change. However, the decrease in the concentration of nitrate due to phytoplankton consumption could be considered as an indirect indicator of physiological adaptation previous to the (potential) biomass

accumulation or bloom. This assertion is stressed by the fact that significant changes in physiological variables derived from process-studies measured on the 2005 cruise, such as the changes in the slope of the photosynthesis–irradiance (P–E) curve, indicating photo-adaptation to a different underwater PAR regime (López-Álvarez *et al.*, submitted for publication), or in sinking speed, suggesting potential buoyancy regulation (Acuña *et al.*, submitted for publication), were concurrent with the change in nitrate concentration reported here. During the 2005 cruise, nitrate concentration dropped 5 days after the increase in solar radiation (Fig. 8B), but biomass remained low during the 4 days that followed the decrease in nitrate. On the 2004 cruise, the situation was different because the increase of solar radiation and the decrease of wind speed occurred almost simultaneously. However, during the first adaptive period, which lasted 6 days, biomass did not accumulate even with the drop in wind speed (Fig. 8B).

During the late-winter and early-spring blooms, the timing and duration of the second lag period (i.e. extrinsic component) depends also on a physical mechanism which maintains cells in the illuminated zone of the water column to make net population growth rate

positive exceeding loss terms such as sedimentation or grazing. Triggering variables for this physically driven phase, the blooming or accumulation phase, are solar radiation, for its role on surface heating and development of the seasonal thermocline (i.e. shoaling of the MLD) (Woods and Barkmann, 1986) and wind, for its prevalent role in the control of water column turbulence (Backhaus *et al.*, 2003; MacKenzie and Leggett, 1993) (Fig. 8A). In 2005, 2 days after the initiation of nitrate consumption, the wind speed decreased and 2 days later the bloom took place, whereas in 2004 the first lag period ended when wind speed was low, and the second lag was very short (1 day) (Fig. 8B). In the late-winter blooms observed in 2004 and 2005, the shoaling of the MLD occurred when the bloom was well underway, while the wind-derived water column turbulence (MacKenzie and Leggett, 1993) decreased before the onset of the bloom. This sequence of events suggests that critical turbulence was the main mechanism causing the onset of the bloom. However, without estimations of critical depth and higher temporal resolution, it is not possible to dismiss the Sverdrup critical depth mechanism acting for instances at daily time scales by changes in the diurnal thermocline through the Woods–Onken mechanism (Woods and Onken, 1982).

Timing of the bloom can be greatly affected by meteorological and hydrographic disturbances. The first lag is externally controlled by means of the effect of light regime on the biochemical adjustments that individual cells must carry out to become competent to grow. The second lag is also externally controlled because its duration is very sensitive to changes in population net growth rate, and any factor influencing it controls the duration of this second lag phase. For instance, in 2004 a meteorological disturbance associated with the passage of a low atmospheric pressure system disrupted surface water stability, making chlorophyll concentrations decrease and nitrate concentration to increase. In this case, the disturbance was short and the previous biomass accumulation was not completely reset; when favourable conditions returned, biomass accumulation re-built. In the same way that a disturbance during the second lag causes the interruption of bloom development by means of its effect on net growth rate, a disturbance during the first lag that interrupts physiological adaptation (e.g. PAR decrease) can delay bloom onset and even return the system to the initial situation. This suggests a characteristic time scale for the development of a bloom. A bloom can be expected to occur when its time scale is short relative to the time between disturbances (Platt *et al.*, 1991). In this work, this time scale was set at 7–9 days for conditions of late-winter in the central Cantabrian Sea. MacIsaac *et al.* (MacIsaac *et al.*,

1985) reported lags of 1–5 days for oceanic phytoplankton under upwelling conditions and Harris (Harris, 1983) reported lags of 11 days for lake phytoplankton under vertical mixing (Duarte, 1990).

This sequential mechanism made up of an adaptive phase and a growth phase, both externally controlled, could explain why the late-winter and spring blooms in the Central Cantabrian Sea, and presumably in other temperate shelf ecosystems, are not unique and uniform events but a succession of short-lived peaks of production and accumulation driven by the meteorological scenario experienced by the phytoplankton populations. Moreover, the same model could be applied not only to light-limited blooms but also to nutrient-limited blooms like those which take place in late summer/early autumn in temperate ecosystems. The environmental triggering change in this case would be the replenishment of nutrients at the surface and the forcing variables would be a mixing event or an upwelling situation; anyhow, an individual adaptive phase would be necessary before the potential biomass accumulation.

CONCLUSIONS

Phytoplankton blooms in the central Cantabrian Sea can take place during late-winter in the absence of water-column stratification, suggesting that critical turbulence is the mechanism allowing bloom development. However, a physical mechanism keeping cells in the euphotic layer of the water-column is a necessary but not sufficient condition for bloom initiation. The elapsed time between the changes in relevant meteorological conditions such as solar radiation and wind speed indicates that some physiological criterion must be taken into account to define a time scale for bloom initiation.

The time scale for the development of a phytoplankton bloom in the central Cantabrian Sea is around 7–8 days. This characteristic time scale can be divided in two periods: one of physiological adaptation, driven by the increase in solar radiation that results in an enhancement of primary production, which in our case lasted around 4–6 days; and another one of growth, driven by the stability of the water column that results in biomass accumulation, which lasted 1–4 days.

Meteorological conditions under which phytoplankton blooms take place act as forcing variables on the bloom onset and determine its development, which can explain why the late-winter and spring blooms in the Central Cantabrian Sea happen as a succession of short-lived peaks of production and accumulation more than a unique and uniform event.

ACKNOWLEDGEMENTS

We thank the captain and crew in the R/V García del Cid for their assistance during the DINAPROFIT0304 and DINAPROFIT0205 cruises. We are indebted to all participants in DINAPROFIT project for their work at sea and in the laboratory. Thanks to Gonzalo González-Nuevo for the time-series analysis. Puertos del Estado (Ministerio de Fomento) provided Cabo Peñas buoy data and E Ronzón kindly provided solar radiation data from his meteorological station in Gijón. NCEP Daily Global Analyses data were provided by the NOAA/OAR/ESRL PSD, Boulder, Colorado, USA, from their web site at <http://www.cdc.noaa.gov/>.

FUNDING

This work was funded by the Ministerio de Ciencia y Tecnología through the DINAPROFIT project (*Dynamics of winter phytoplankton blooms in the Central Cantabrian Sea*, MCT-03-REN09549-C0301). The work of Eva Álvarez is supported by a *Severo Ochoa* PhD grant from the Plan de Ciencia, Tecnología e Innovación (PCTI) 2006–2009 from the Gobierno del Principado de Asturias.

REFERENCES

- Azam, F., Fenchel, T., Field, J. G. *et al.* (1983) The ecological role of water-column microbes in the sea. *Mar. Ecol. Prog. Ser.*, **10**, 257–263.
- Backhaus, J. O., Wehde, H. and Hegseth, E. N. (1999) ‘Phyto-convection’: the role of oceanic convection in primary production. *Mar. Ecol. Prog. Ser.*, **189**, 77–92.
- Backhaus, J. O., Hegseth, E. N., Wehde, H. *et al.* (2003) Convection and primary production in winter. *Mar. Ecol. Prog. Ser.*, **251**, 1–14.
- Calvo-Díaz, A., Morán, X. A. and Suárez, L. A. (2008) Seasonality of picophytoplankton chlorophyll *a* and biomass in the central Cantabrian Sea, southern Bay of Biscay. *J. Mar. Syst.*, **72**, 271–281.
- Dale, T., Rey, F. and Heimdal, B. R. (1999) Seasonal development of phytoplankton at a high latitude ocean site. *Sarsia*, **84**, 419–435.
- Duarte, C. M. (1990) Time lags in algal growth: generality, causes and consequences. *J. Plankton Res.*, **12**, 873–883.
- Eilertsen, H. C. (1993) Spring blooms and stratification. *Nature*, **363**, 24.
- Falkowski, P. G., Dubinsky, Z. and Wyman, K. (1985) Growth-irradiance relationships in phytoplankton. *Limnol. Oceanogr.*, **30**, 311–321.
- Fernández, E. and Bode, A. (1991) Seasonal patterns of primary production in the Central Cantabrian Sea (Bay of Biscay). *Sci. Mar.*, **55**, 629–636.
- Gran, H. H. and Braarud, T. (1935) A quantitative study of the Phytoplankton in the Bay of Fundy and the Gulf of Maine. *J. Biol. Board Can.*, **1**, 279–467.
- Grashoff, K., Ehrhardt, M. and Kremling, K. (1983) *Methods of Seawater Analysis*, 2nd edn. Verlag Chemie, Weinheim.
- Harris, G. P. (1983) Mixed layer physics and phytoplankton populations: studies in equilibrium and non-equilibrium ecology. In Round, F. E. and Chapman, D. J. (eds), *Progress in Phycological Research* Vol. 12. Elsevier, Amsterdam, pp. 1–52.
- Henson, S. A., Robinson, I., Allen, J. T. *et al.* (2006) Effect of meteorological conditions on interannual variability in timing and magnitude of the spring bloom in the Irminger Basin, North Atlantic. *Deep-Sea Res. I*, **53**, 1601–1615.
- Huisman, J., van Oostveen, P. and Weissing, F. J. (1999) Critical depth and critical turbulence: two different mechanisms for the development of spring phytoplankton blooms. *Limnol. Oceanogr.*, **44**, 1781–1787.
- Ibanez, F., Fromentin, J.-M. and Castel, J. (1993) Application of the cumulated function to the processing of chronological data in oceanography. *Cr. Acad. Sci. Paris (Sci. Vie)*, **316**, 745–748.
- Legendre, L. (1990) The significance of microalgal blooms for fisheries and for the export of particulate organic carbon in oceans. *J. Plankton Res.*, **12**, 681–699.
- Levitus, S. (1982) Climatological Atlas of the World Ocean. *NOAA/ERL GFDL Professional Paper 13*, Princeton, NJ, 173 pp.
- Longhurst, A. R. (1998) *Ecological Geography of the Sea*. Academic Press, San Diego, 398 pp.
- MacIsaac, J. J., Dugdale, R. C., Barber, R. T. *et al.* (1985) Primary production cycle in an upwelling center. *Deep-Sea Res.*, **32**, 503–529.
- MacKenzie, B. R. and Leggett, W. C. (1993) Wind-based models for estimating the dissipation rates of turbulent energy in aquatic environments: empirical comparisons. *Mar. Ecol. Prog. Ser.*, **94**, 207–216.
- Nogueira, E., Ibanez, F. and Figueiras, F. G. (2000) Effect of meteorological and hydrographic disturbances on the microplankton community structure in the Ría de Vigo (NW Spain). *Mar. Ecol. Prog. Ser.*, **203**, 23–45.
- Peliz, A., Dubert, J., Santos, A. M. P. *et al.* (2005) Winter upper ocean circulation in the Western Iberian Basin—Fronts, Eddies and Poleward Flows: an overview. *Deep-Sea Res. I*, **52**, 621–646.
- Platt, T., Bird, D. F. and Sathyendranath, S. (1991) Critical depth and marine primary production. *Proc. R. Soc. Lond. B*, **246**, 205–217.
- Riley, G. A. (1942) The relationship of vertical turbulence and spring diatom flowerings. *J. Mar. Res.*, **5**, 67–87.
- Siegel, D. A., Doney, S. C. and Yoder, J. A. (2002) The North Atlantic spring phytoplankton bloom and Sverdrup’s critical depth hypothesis. *Science*, **296**, 730–733.
- Smayda, T. J. (1998) Patterns of variability characterizing marine phytoplankton, with examples from Narragansett Bay. *ICES J. Mar. Sci.*, **55**, 562–573.
- Smetacek, V. and Passow, U. (1990) Spring bloom initiation and Sverdrup’s critical-depth model. *Limnol. Oceanogr.*, **35**, 228–234.
- Sverdrup, H. U. (1953) On conditions for the vernal bloom of phytoplankton. *J. Cons. Perm. Int. Explor. Mer.*, **18**, 287–295.
- Tilstone, G. H., Figueiras, F. G., Lorenzo, L. M. *et al.* (2003) Phytoplankton composition, photosynthesis and primary production during different hydrographic conditions at the Northwest Iberian upwelling system. *Mar. Ecol. Prog. Ser.*, **252**, 89–104.
- Thompson, R. O. R. Y. (1976) Climatological models of the surface mixed layer on the ocean. *J. Phys. Oceanogr.*, **6**, 496–503.

- Townsend, D. W., Keller, M. D., Sieracki, M. E. *et al.* (1992) Spring phytoplankton blooms in the absence of vertical water column stratification. *Nature*, **360**, 59–62.
- Ueyama, R. and Monger, B. C. (2005) Wind-induced modulation of seasonal phytoplankton blooms in the North Atlantic derived from satellite observations. *Limnol. Oceanogr.*, **50**, 1820–1829.
- Utermöhl, H. (1958) Zur Vervollkommnung der quantitativen Phytoplankton-Methodik. *Mitt. int. Ver. theor. angew. Limnol.*, **9**, 1–38.
- Varela, M. (1996) Phytoplankton ecology in the Bay of Biscay. *Sci. Mar.*, **60**, 45–53.
- Woods, J. D. and Barkmann, W. (1986) The influence of solar heating on the upper ocean. I. The mixed layer. *Q. J. R. Meteorol. Soc.*, **112**, 1–27.
- Woods, J. D. and Onken, R. (1982) Diurnal variation and primary production in the ocean: preliminary results of a Lagrangian ensemble model. *J. Plankton Res.*, **4**, 735–756.